AGRISCIENCE AND TECHNOLOGY
Armenian National Agrarian University
ԱԳՐՈԳԻՏՈՒԹՅՈՒՆ ԵՎ ՏԵԽՆՈԼՈԳԻԱ АГРОНАУКА И ТЕХНОЛОГИЯ
International Scientific Journal
ISSN 2579-2822

OPEN ACCESS
UDC 631.3
doi: 10.52276/25792822-2025.2-112

Justification of the Stability Parameters for the Turning Motion of a Horticultural Robotic Platform

Arshaluys Tarverdyan, Artur Altunyan, Albert Grigoryan
Armenian National Agrarian University
arshaluystar@gmail.com, artur_altunyan@mail.ru, algrig1968@mail.ru

ARTICLE INFO

Keywords:
dynamic analysis,
horticultural robot,
kinematic analysis,
running gear,
software parameters

Conflict of Interest
The authors declare no conflict of interest concerning the research, authorship, and/or publication of this article.

ABSTRACT

The article discusses the issue related to the development of a multifunctional horticultural robot platform. The previous article in this series substantiated the necessity of designing a robot platform for integrated cultivation of inter-row, inter-tree (inter-vine), and near-trunk areas in vineyards and orchards, taking into account the specific soil and climatic conditions of the Republic of Armenia.A structural schematic of the robot platform has been developed, and a kinematic analysis has been conducted, the results of which served as the basis for programming the robot›s control system. Tests of the prototype of the developed robot platform demonstrated that, in order to create a fault-free, four-wheeled robot platform with independently controlled wheels, additional kinematic and dynamic studies are required. As a result of the conducted analyses, mathematical expressions were derived that enabled adjustments to be made in the robot platform's control software with respect to its kinematic parameters. Specifically, the program for controlling the robot platform's turning motion now accounts not only for the correlation between the wheel axes' rotation angles around the vertical axis, but also for those between the angular velocities of the wheels rotating around their own axes. The dynamic studies produced accurate expressions for determining lateral forces, which will enable the development of the robot platform's running and suspension systems that not only minimize soil damage but also ensure high operational reliability and durability.

Introduction

Over the past decade, the trends in the development of agricultural production in all countries have been shaped by one of the most critical global challenges facing humanity—the need to meet the growing demand for food products. Addressing this challenge necessarily implies the preservation and improvement of land resources, compliance with environmental requirements, an increase in production volumes, the production of environmentally friendly products, the complete mechanization of agricultural production, and—most crucially today—the reduction of energy consumption in performing these tasks (Bak, 2003; Abrosimov, 2022).

It is evident that the comprehensive resolution of this issue is objectively limited when relying solely on existing technologies and technical means. The various sensors and detectors used in fieldwork are quite expensive and generally inaccessible to farmers, particularly in large quantities. Soil analysis is mostly performed manually, and disease observation and assessment require the direct involvement of an agronomist (Abrosimov, 2022).

This is perhaps the reason why two fundamental trends have recently come to the forefront of technological processes in agricultural production worldwide:

- The most prominent and relevant direction of the past decade in agricultural production has been precision agriculture, which is scientifically grounded in the objective fact that even within the boundaries of a single field, significant heterogeneity exists. To detect, record, and assess these heterogeneities, advanced technologies are used, including global positioning systems (GPS, GLONASS, Galileo), specialized sensors, aerial photography, and agro-management software based on geographic information systems (GIS) (Abrosimov, 2022).
- The second direction, without which it is impossible to effectively utilize the data obtained from the aforementioned technologies, is robotized farming. This means that agricultural production must transition toward the cultivation of crops that are comparatively easier to manage using robotic systems, including for harvesting operations. This, in turn, necessitates a specialized approach to the design of fields, which significantly facilitates the development of agricultural robots (Bak, 2003; Zagazezheva, 2021; Skvortsov, 2018).

The stages of robotics development, the rapidly increasing scale of its application in agricultural production, the expansion of functional capabilities, and the technical and agro-technological requirements associated with these advancements were thoroughly discussed in a previous study (Tarverdyan, 2024). The mentioned article, demonstrated that a critical aspect—namely, the development of the running gear—requires further investigation.

For the proposed robot platform, a fundamentally new running gear and suspension system is being developed. To perform the necessary calculations for this system, it is essential to determine the vertical and tangential components of the forces acting on the wheels.

Though the global robotics market is developing at an unprecedented pace—having expanded nearly twentyfold over the past five years (Bak, 2003; Godin, 2020; Exclusive Report, 2024; Navone, 2025, Fountas, 2020)—their application in Armenia's agricultural sector remains highly limited. This is largely due to the high market cost of such technologies, making them inaccessible to most local business entities/producers. Additionally, the structural features of existing robotic systems are designed for other soil and climatic conditions, and their operational reliability is relatively low when used on Armenia's soil types (Tillett, 1991; Tarverdyan, 2024).

These circumstances suggest that the issue can be addressed in one of two ways: either by making structural modifications to existing robots or by developing a new, cost-effective, and universal robot platform that is better adapted to the local terraincharacterized by the presence of stones of various sizes and a rugged relief.

For all agricultural mobile robots, the mobile platform is a critical component that plays a significant role in the overall performance of the system.

Researchers have focused much of their efforts on the development of robust mobile platforms for agricultural robots [Qiu et all, 2018], as well as on improving their control and positioning accuracy, since these aspects are essential and fundamental in precision agriculture [Lipiński et all, 2016; Bayar et all, 2015].

Among the various agricultural mobile platforms, the four-wheel independent drive (4WID) configuration represents the most widely used kinematic solution. The 4WID configuration provides high mobility flexibility to the mobile platform, while simultaneously increasing the complexity of coordinated motion control. For this reason, some researchers often prefer a four-wheel-driven configuration in which the four wheels are not independently steered; instead, a mechanical steering linkage is established between the front and rear wheel pairs, meaning that these wheel pairs are mechanically coupled through a steering mechanism (Qiu et all, 2018; Akimov, 2017; Blasco, 2002; Cho, 2002).

The conceptual design of the proposed robot platform is based on the technical-technological requirements applied to modern agricultural robots. It consists of the following main systems: a base platform with four independently driven and controlled wheels and suspension units; an

electronic computer-based control unit; and various tools and implements for executing a wide range of agro-technological operations (Bak, 2003; Tarverdyan, 2024; Toda, 1998; Orebäck, 2003; Cho, 2002).

The present article discusses the results of the kinematic and dynamic analysis of the robot platform's running gear, aimed at accurately determining the parameters necessary for the robot's development

Materials and methods

As previously mentioned, for the robot-platform intended as a transport vehicle for performing agrotechnological operations, the preferred configuration is a four-wheel drive system with independently controlled wheels. The platform's ability to move smoothly in parallel directions allows for high maneuverability in certain scenarios, eliminating the need for turning maneuvers.

Though the use of four independently controlled wheels results in a non-linear vehicle behavior and makes control less straightforward, given the relatively low operational speeds (2–6 km/h), even simple control systems can be effective (Agricultural Robots Market Worth $11.9 Billion by 2026 – Exclusive Report by Markets, Tarverdyan, 2024; Cho, 2002).

A schematic diagram of the proposed and under-development robot-platform is presented in Figure 1. The system consists of: 1. a frame-platform to which various devices and tools for performing agrotechnological operations can be attached; 2. four independently driven and controlled motorized wheels; 3. an electronic control system for managing the movement of the drive wheels;4. a mechanism for steering the wheels; and, 5. a pneumo-hydraulic damping suspension system.

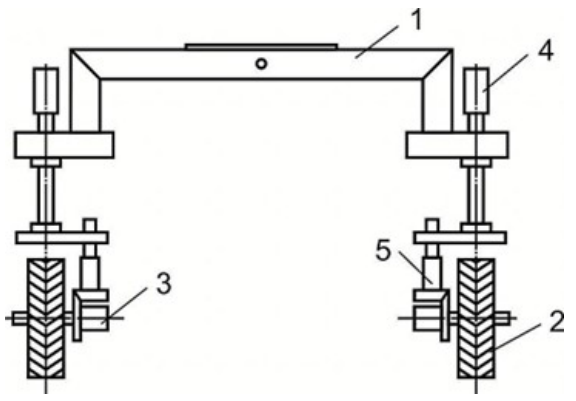

Figure 1. Schematic diagram of the running gear of the proposed robot-platform *(composed by the authors)*.

The electronic-computerized wheel module controls the rotation (axial turning) of the wheels around a vertical axis, based on a software algorithm for the kinematic correlation of the wheel turning angles. It also manages the torque (or current) of the electric motors driving the four wheels. The servo-drive electronics used for steering control provide feedback based on the turning angle of rotation. This is a fundamental principle in the structural scheme of agrorobots (Bak, 2003; Torii, 2000; Toda, 1999; Litvinov, 1971).

As previously mentioned, the first step in the development and design of the agrorobot was to identify the relationship and values of the kinematic parameters of steady motion and turning that would eliminate lateral wheel slippage—a highly undesirable phenomenon.

The robot-platform's straight parallel motion is achieved and maintained in a stable condition through software-supported control and synchronization of the same torque and angular velocity on all four independently driven wheels. As for the turning motion of the robot-platform, it presents particular interest from the perspective of the issue under discussion.

A schematic of the robot-platform's turning motion using all steerable wheels is presented in Figure 2.

The previous article (Tarverdyan, 2024) presented the results of the kinematic analysis of the robot-platform's drive module/running gear. Specifically, the relationship of the wheel turning angles was derived:

$$ctg\theta_1 - ctg\theta_2 = \pm\frac{2B}{L}, \qquad (1)$$

where θ_1 is the steering/turning angle of the outer wheel on the front axle ($\theta_1=\theta_3$, θ_3 *is is the steering angle of the outer wheel on the rear axle)*, θ_2 is the steering angle of the inner wheel on the front axle($\theta_2=\theta_4$, θ_4 *is the steering angle of the inner wheel on the rear axle*). The relationship between θ_1 *and* θ_2 expressed in equation (1), forms the basis for programming the control model of the robot-platform's turning motion.

The average turning angle and angular velocity of the turn have also been determined:

$$tg\alpha = \frac{L}{2R} \;\; and \;\; \omega = \frac{V}{R} = \frac{V \cdot 2tg\alpha}{L}. \qquad (2)$$

The diagram of the forces acting on the wheels of the robot platform during turning (Fig. 2.b) has been discussed, and expressions for determining the slip angles of the wheels have been derived.

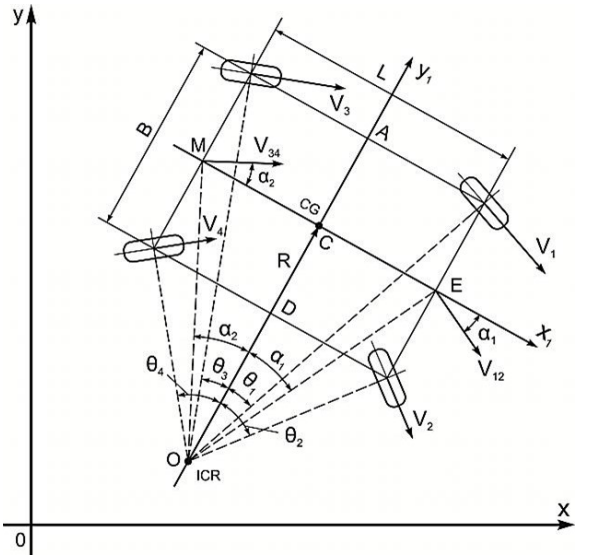

Figure 2. Kinematic diagram of the all-wheel-steering robot platform's turning *(composed by the authors)*.

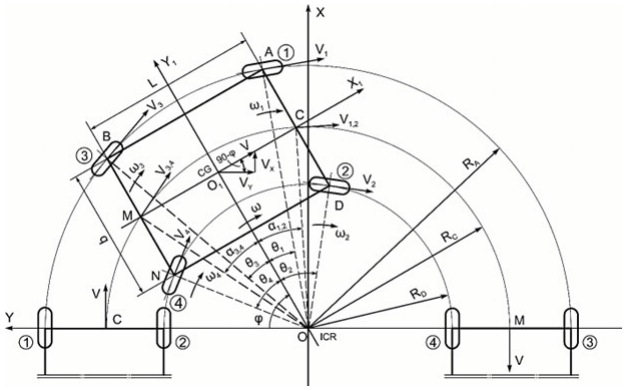

Figure 3. Diagram for determining the angular velocities of the robot platform's wheels during turning *(composed by the authors)*.

$$\varepsilon_1 = \frac{m\upsilon^2}{R'} \cdot \frac{b}{L \cdot K_1} \text{ and } \varepsilon_2 = \frac{m\upsilon^2}{R'} \cdot \frac{a}{L \cdot K_2}. \quad (3)$$

It has been established that, given the geometric and kinematic parameters of the robot platform under development and design, and assuming the use of rigid wheels, the slip angles of the wheels are approximately 15 times smaller than the average turning angle (Tarverdyan, 2024).

However, it should be noted that tests of the prototype model of the robot platform revealed a significant deviation between the theoretically obtained and experimental data, which naturally implies the need for further research to refine the values used in the programming of the control system.

Results and discussions

As already mentioned, preliminary tests of the prototype model of the robot platform under development showed that, during turning, incorporating the relationship between the rotation angles of the inner and outer wheels into the programming of the driving system is important but not sufficient for developing and designing a reliable driving mechanism that ensures high maneuverability and eliminates the phenomenon of wheel slip. This aspect becomes extremely important, as the resulting optimal parameters are used as the basis for programming the control systems of the robot platform's driving mechanism.

Since all four wheels of the robot platform are controlled independently in terms of both the driving torques applied to the wheel axles and their rotation angles around the vertical axis during turning, the angular velocities of each wheel's rotation around its own axis must also be programmatically controlled.

Otherwise, slippage and spinning/skidding in place may occur, which has a highly negative effect— not so much in terms of potential damage to the soil, but rather due to unacceptable deformations and wear of the driving system components, thereby undermining operational reliability and durability.

Let us assume that the robot platform makes its turn at the end of rows of trees or other crops along a circular arc with a constant velocity V, which is equal to the speed of the aggregate's linear motion (Figure 3).

The angular velocity of the turn is: $\omega = \frac{V}{R_c} \cdot$ Considering that in the case of four steerable wheels, during turning: $V_1=V_3=\omega \cdot R_A$ and $V_2=V_4=\omega \cdot R_D$, the angular velocities of the wheels around their own axes will be:

$$\omega_1 = \omega_3 = \frac{V_1}{r}, \quad \omega_2 = \omega_4 = \frac{V_2}{r}, \quad or$$
$$\omega_1 = \frac{\omega R_A}{r}; \quad \omega_2 = \frac{\omega R_D}{r}, \quad (4)$$

where r is the radius of the outer ring of the wheels.

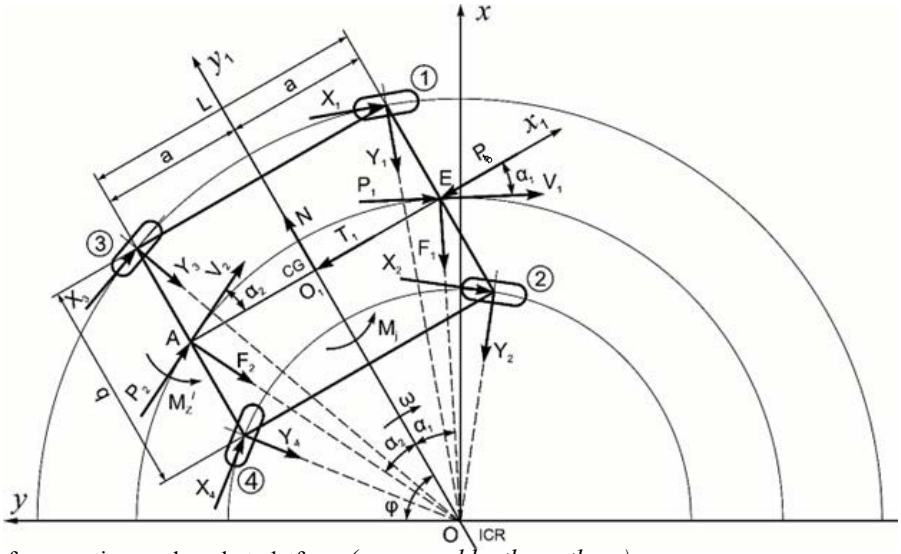

Figure 4. Diagram of the forces acting on the robot platform *(composed by the authors)*.

According to the diagram (Fig. 3):

$$R_A=R_c+0.5B;\ \ R_D=R_c-0.5B \text{ or}$$

$$R_A=0.5Lctg\theta_1;\ \ R_D=0.5Lctg\theta_2.$$

Therefore:

$$\left.\begin{aligned}\omega_1 &= \frac{\omega\cdot 0.5Lctg\theta_1}{r}\\ \omega_2 &= \frac{\omega\cdot 0.5Lctg\theta_2}{r}\end{aligned}\right\}, \qquad (5)$$

the relationship between will be:

$$M_j = m\rho^2\frac{d\omega}{dt}. \qquad (6)$$

In addition to expression (1), expression (6) must also be incorporated into the programming base.

To determine the force factors acting on the driving system of the robot platform, an analysis was carried out of the forces acting on the wheels, and consequently on the frame during turning.

The task is reduced to determining the total lateral reaction forces F_1 and F_2 acting on the conditionally defined front and rear wheels.

The diagram of the forces acting on the robot platform in the horizontal plane is presented in Figure 4.

During turning, the robot platform is subject to several forces: the tangential forces of all four wheels - X_1, X_2, X_3 and X_4, which result from the driving torques generated by the motors; the lateral (slip) forces of the wheels Y_1, Y_2, Y_3 and Y_4; the normal and tangential components of the inertial forces - N and T; the resultant torque caused by the differences in forces acting on the wheels - $X_i = M_m\frac{K\cdot i_0\cdot\eta}{r_k}$, and the inertial moment - M_j.

The resultant of the tangential forces (X_i) at the contact surface between the wheels and the ground is determined as follows (Litvinov, 1971):

$$X_i = M_m\frac{K\cdot i_0\cdot\eta}{r_k}, \qquad (7)$$

where M_m is the driving torque developed by the motor (Nm); K is the torque distribution coefficient (in this case, $K = 1$, as the motors driving the wheels are of equal power and operate independently); i_0 is the gear ratio, in case of direct transmission , $i_0=1$, η- is the transmission efficiency; r_k is the radius of the wheel (in meters).

As mentioned above in the case of rigid wheels, the slip angle (ε) is significantly smaller than the average turning angle (α). Taking this into account, the forces X_1 and X_2, as well as X_3 and X_4, can be represented with their respective resultants P_1 and P_2, which can be applied at points E and A of the frame, respectively. Specifically: $P_1=X_1+X_2$; $P_2=X_3+ X_4$. Using the same logic, the resultant lateral forces (F_1 and F_2) can also be applied at the corresponding points.

To identify the phenomenon of lateral slipping of the robot platform's wheels during turning, it is necessary to examine the conditions of its relative equilibrium. In this context, equilibrium refers to a stable and uniform motion regime.

Let us consider the equilibrium conditions in the coordinate system x_1, o_1, y_1, where the origin is aligned with the center of gravity (CG), x_1 and y_1 axes coincide with the longitudinal and transverse axes of the platform. The equilibrium equations will be:

$$\Sigma X_1=0;\ P_1Cos\alpha_1-F_1sin\alpha_1-T+P_2Cos\alpha_2+F_2sin\alpha_2=P_b. \quad (8)$$

$$\Sigma Y_1=0;\ N-P_1sin\alpha_1-F_1Cos\alpha_1+P_2sin\alpha_2-F_2Cos\alpha_2=0. \quad (9)$$

$\Sigma M_z=0$; (Z axis passes through point o_1 and is perpendicular to the $x_1\ o_1\ y_1$ plane),

$$M_z'+M_j-P_1asin\alpha_1-F_1aCos\alpha_1-P_2asin\alpha_2+F_2aCos\alpha_2=0. \quad (10)$$

In the case of the robot platform's presented diagram and rigid wheels, we can assume that: $\alpha_1=\alpha_2=\alpha$, $P_1=P_2=P$, $F_1=F_2=F$. In that case, expressions (8), (9) and (10) will take the following forms:

$$2Pcos\alpha-T=P_b. \quad (11)$$

$$N-2F_1cos\alpha=0. \quad (12)$$

$$M_z'+M_j-2Pasin\alpha=0. \quad (13)$$

In the last three expressions, it is necessary to present the force components M_z'; M_j; N and T in explicit form.

The moment M_z' results from the parallel displacement of the driving tangential forces of the four driving wheels (X_1, X_2, X_3 and X_4) from their original points of application to points E and A.

As a result of this parallel displacement of forces, additional moments are generated, the values of which will be as follows (see Figs. 3 and 4):

$$\begin{aligned} M'_{z1}&=-X_1\frac{B}{2}\cos\theta_1; \quad M'_{z2}=-X_2\frac{B}{2}\cos\theta_2;\\ M'_{z3}&=-X_3\frac{B}{2}\cos\theta_3; \quad M'_{z4}=-X_4\frac{B}{2}\cos\theta_4. \end{aligned} \quad (14)$$

Considering that the vectors X_1, X_2, X_3 and X_4 are equal in modules, in the moment expressions (14), we can assume them to be equal to each other and denote them as X. Additionally $\theta_1=\theta_3$; $\theta_3=\theta_4$. The total moment M_z' will be determined by the following expression:

$$M_z'=XB(cos\theta_2-cos\theta_1). \quad (15)$$

The inertial moment (M_j) acting on the robot-platform during the turn is determined by the following well-known expression:

$$M_j=m\rho^2\frac{d\omega}{dt}, \quad (16)$$

where m is the total mass of the robot-platform ($m=\frac{G}{g}$, where G is the weight of the robot-platform), ρ is the radius of gyration of the robot-platform's mass m with respect to the vertical axis (Z), $\frac{d\omega}{dt}$ - is the angular acceleration of the robot-platform in the turning zone (in the general solution of the problem, it is assumed that the robot-platform is moving with acceleration).

The inertial forces N and T are determined by the products of the robot-platform's mass (m) and the normal and tangential accelerations of the center of gravity (CG).

The acceleration components of the gravity center have been determined by considering the platform's motion along a circular arc as a rotational movement around the center O within the xOy coordinate system (Figs. 3 and 4). Let us assume that in the current position, the radius from the origin to the center of gravity (OCG) has rotated by an angle φ relative to its initial position (Figs. 3 and 4); in that position, the velocity vector V forms an angle of ($90°-\varphi$) with the Oy axis.

The components of velocity (V) along the y and x axes will be:

$$V_y=V\sin\varphi;\ V_x=V\cos\varphi. \quad (17)$$

Considering that the angular velocity is $\omega=\frac{d\varphi}{dt}$ and the angular acceleration is $\varepsilon=\frac{d\omega}{dt}$, by differentiating expressions (17), we obtain the components of the acceleration of the gravity center.

$$\left.\begin{aligned} W_y&=\frac{dV_y}{dt}=\frac{dV}{dt}\sin\varphi+V\cdot\omega\cdot\mathrm{Cos}\,\varphi\\ W_x&=\frac{dV_x}{dt}=\frac{dV}{dt}\mathrm{Cos}\,\varphi-V\cdot\omega\cdot\sin\varphi \end{aligned}\right\}. \quad (18)$$

By projecting the acceleration components along the y and x axes onto the X_1 and y_1 axes passing through the platform's center of gravity (O_1, or CG), we obtain:

$$\left.\begin{aligned} W_n &= W_y \cos\varphi - W_x \operatorname{Cos}(90-\varphi) \\ W_t &= -W_y \operatorname{Cos}(90-\varphi) - W_x c\operatorname{os}\varphi \end{aligned}\right\}. \quad (19)$$

Substituting the values of W_y and W_x from expressions (18) into (19), and after transformations, we obtain:

$$\left.\begin{aligned} W_n &= V\cdot\omega \\ W_t &= -\frac{dV}{dt} \end{aligned}\right\}. \quad (20)$$

It should be noted that the 'sign' of W_t is determined by the nature of the motion—whether it is accelerating or decelerating—but in the problem under consideration, it does not play any role, as it has no effect on the lateral forces.

In the general case, for the inertial forces, we will have:

$$N=m\omega v; \quad T=\pm m\frac{dV}{dt}\cdot \quad (21)$$

After determining the force factors, by considering the equilibrium conditions of the system with respect to the vertical axes passing through points A and E of the platform (Fig. 4), we determine the lateral forces F_1 and F_2:

$$\Sigma M_{z(A)}=M_z'+M_j+Na-F_1 L\cos\alpha-P_1 L\sin\alpha=0,$$

wherefrom:

$$F_1=\frac{M_z'+M_j+Na-P_1 L\sin\alpha}{L\cos\alpha}. \quad (22)$$

$$\Sigma M_{z(E)}=M_z'+M_j-Na-P_2 L\sin\alpha+F_2 L\cos\alpha=0,$$

wherefrom:

$$F_2=\frac{Na+P_2 L\sin\alpha-M_z'-M_j}{L\cos\alpha}. \quad (23)$$

The slip angles of the front and rear wheels of the robot-platform will be:

$$\varepsilon_1=K\cdot F_1;\ \ \varepsilon_2=K\cdot F_2,$$

where K is the slip coefficient of the wheels.

Thus, as a result of a more detailed force analysis of the robot-platform, refined expressions (22) and (23) have been obtained for determining the lateral forces of the wheels, which will make it possible to introduce appropriate adjustments in the programming process of the running gear control system, with the aim of reducing the lateral forces acting on the running gear.

Conclusions

1. To achieve stable turning performance of the multifunctional horticultural robot platform, independent wheel-control programming is required. The control logic is defined strictly by analytical relationships between the wheel-steering angles and their angular velocities.
2. Dynamic analysis of the platform's turning motion yielded analytical expressions that guide for designing of the chassis and suspension system. These results eliminate wheel lateral skidding and ensure reliable and durable operation.

References

1. Abrosimov, V.K., Raykov, A.N. (2022). Intelligent Agricultural Robots. Moscow: Career Press, 5126 (in Russian).
2. Agricultural Robots Market worth $11.9 billion by 2026-Exclusive Report by Markets-2021. https://www.,bloomberg.com/press-releases/2021-11-09/agricultural-robots-market-worth-11-9-billion-by-2026-exclusive-report-by-marketsandmarkets (accessed on 16.10.2024).
3. Akimov, A.V. (2017). Robotics and labor-saving technologies: perspectives of impact on socioeconomic development. Historical psychology and sociology of history. - No 1. - pp. 173-192 (in Russian).
4. Bak, T., & Jakobsen, H. (2004). Agricultural robotic platform with four wheel steering for weed detection. Biosystems Engineering, 87(2), 125-136. https://doi.org/10.1016/j.biosystemseng.2003.10.009.
5. Bayar, G., Bergerman, M., Koku, A. B., & Ilhan Konukseven, E. (2015). Localization and control of an autonomous orchard vehicle. Computers and Electronics in Agriculture, 115, 118-128, https://doi.org/10.1016/j.compag.2015.05.015.
6. Blasco, J., Aleixos, N., Roger, J. M., Rabatel, G., & Moltó, E. (2002). AE - Automation and emerging technologies: Robotic weed control using machine vision. Biosystems Engineering, 83(2), 149-157.
7. Cho, S. I., Kim, Y.Y., An, K.J. (2002). Development of a three-degrees-of-freedom robot for harvesting lettuce using machine vision and fuzzy logic control. Biosystems Engineering, 82(2), 143-149.

8. Fountas, S., Mylonas, N., Malounas, I., Rodias, E., Hellmann Santos, C., & Pekkeriet, E., (2020). Agricultural Robotics for Field Operations. Sensors, 20(9), 2672. https://doi.org/10.3390/s20092672.

9. Godin, V.V., Belousova, M.N., Belousov, V.A., Terekhova, A.E. (2020). Agriculture in the digital age: challenges and solutions. E-Management. - No. 3(1), - pp. 4-15 (in Russian).

10. Lipiński, A. J., Markowski, P., Lipiński, S., & Pyra, P. (2016). Precision of tractor operations with soil cultivation implements using manual and automatic steering modes. Biosystems Engineering, 145, 22-28., https://doi.org/10.1016/j.biosystemseng.2016.02.008.

11. Litvinov, A.S. (1971). Vehicle Controllability and Stability. Moscow: Machinery Construction (Mashinostroenie). Publishing House, - 416 p. (in Russian).

12. Navone, A., Martini, M., & Chiaberge, M. (2025). Autonomous Robotic Pruning in Orchards and Vineyards: a Review. arXiv preprint arXiv:2505.07318. https://doi.org/10.1016/j.atech.2025.101283.

13. Orebäck, A., & Christensen, H. I. (2003). Evaluation of architectures for mobile robotics. Autonomous robots, 14(1), 33-49.

14. Qiu, Q., Fan, Z., Meng, Z., Zhang, Q., Cong, Y., Li, B., ... & Zhao, C. (2018). Extended Ackerman Steering Principle for the coordinated movement control of a four wheel drive agricultural mobile robot. Computers and Electronics in Agriculture, 152, 40-50, https://doi.org/10.1016/j.compag.2018.06.036.

15. Skvortsov, E.A., Skvortsova, E.G., Sandu, I.S., Iovlev, G.A. (2018). The transition of agriculture to digital, intelligent and robotic technologies. Economy of the region. - Vol. 14. Issue. 3, - pp. 1014-1028 (in Russian).

16. Tarverdyan, A., Grigoryan, A., & Altunyan, A. (2024). Justification of the Software Kinematic Parameters of a Horticultural Autonomous Robotic Platform. AgriScience and Technology, 4(88), 284-290.

17. Tillett, N. D. (1991). Automatic guidance sensors for agricultural field machines: a review. Journal of agricultural engineering research, 50, 167-187.

18. Toda, M., Kitani, O., Okamoto, T., & Torii, T. (1999). Navigation method for a mobile robot via sonar-based crop row mapping and fuzzy logic control. Journal of Agricultural Engineering Research, 72(4), 299-309. https://doi.org/10.1006/jaer.1998.0371.

19. Torii, T. (2000). Research in autonomous agriculture vehicles in Japan. Computers and electronics in agriculture, 25(1-2), 133-153.

20. Zagazezheva, O. Z., & Berbekova, M. M. (2021). The main trends in the development of robotic technologies in agriculture. Izvestiya KBNTS RAS, (5), 103. https://doi.org/10.35330/1991-6639-2021-5-103-11-20.

Received on 06.03.2025
Revised on 23.05.2025
Accepted on 30.06.2025